Chapter 2

A Semiempirical Approach for a Rapid Comprehensive Evaluation of the Electrophoretic Behaviors of Small Molecules in Free Zone Electrophoresis

Philippe Schmitt-Kopplin and Agnes Fekete

Abstract

A phenomenological model is proposed for the evaluation of relative electrophoretic migration of charged substances present in mixtures and for the rapid pH optimization prior CZE method development. The simple and robust model is based on the Offord model that takes account of the chemical structure. The effective charge and the molecular mass of the molecule are needed; the charge can easily be calculated from pK_a obtained from known sources or simulated with existing pK-calculation programs. A first example was chosen with the separation of hydroxy-s-triazines to illustrate the applicability of this simple approach for determination of the first buffer-pH conditions prior experimental method optimization when separation of different ions is needed. In a second example, the confirmation of aminoalcohols in the CZE method development of unsaturated hexahydro-triazines and oxasolidines.

Key words Semiempiric model, Mobility simulation, Separation optimization, S-triazines, Aminoalcohols, Formaldehyde releasers

1 Introduction

Especially within the fields of *Genomics, Proteomics,* and *Peptidomics*, models for a better understanding of the free zone electrophoresis of DNA fragments (few bp up to several thousands of bp), proteins, or peptides were developed. These models intended an optimization of the separation conditions, a prognosis of electrophoretic separations of these mixtures, and identification of structures based on standardized experimental separation conditions (i.e., small peptide structures obtained after tryptic digestion) [1–5].

Since the introduction of CE in the 1980s, different simulations of the capillary zone electrophoretic processes were proposed. Some of the simulations aimed at the evaluation of equilibrium (binding toward ions and mobility pH dependency) in CZE [6] and can also be used for optimization of separation parameters [7, 8]. Others principally aimed at understanding peak

Philippe Schmitt-Kopplin (ed.), *Capillary Electrophoresis: Methods and Protocols*, Methods in Molecular Biology, vol. 1483,
DOI 10.1007/978-1-4939-6403-1_2,

anomaly/shape [9], peak sharpening effects [10], anomalous spikes, boundary structures using the Kohlrausch regulating function [11], and allow correct interpretation of experimental CZE results [12]. A last approach allowed the determination of physical–chemical parameters that can be deduced from the electrophoretic behavior under variable experimental conditions (dissociation constants pK_a [13, 14], isoelectric points pI [14], hydrophobicities Log(P) [15], charge [16, 17], binding constants [18]).

We propose to simulate electrophoretic mobilities with a *simple and robust guideline for a rapid method development in CE* based on a model involving easily accessible structural data of the analyte (pK, molecular mass). On the other hand, screening of unknown components through a series of CE experiments at different pH allows the evaluation determination of charge variations of these analytes. The proposed model was verified for low molecular weight components.

2 Semiempirical Models

Semiempirical models were already described from the mid-sixties to predict the mobilities of peptides in electrophoretic separation systems and to obtain information on their amide groups [19]. These descriptions were rapidly adapted to capillary electrophoretic separations of polypeptides and proteins [20]. The effective mobility of an analyte can be generally described with a charge-to-size model where the size of the molecules is approximated by their molecular mass M. It was found to be a continuous function of $M^{-1/3}$ to $M^{-2/3}$, depending on the magnitude of M and the ionic strength of the buffer.

The mobility of an analyte in free solution is defined as the ratio of its electric charge Z (Z= q.e, with e the charge on an electron and q the valency) to its electrophoretic friction coefficient f (Eq. 1).

$$\mu = \frac{qe}{f} \tag{1}$$

All models are based on Eq. 1, with two parameters needing to be estimated: the net charge and the frictional coefficient.

$$\zeta = \frac{Z}{4\pi\varepsilon R\left(1+\kappa R\right)} \tag{2}$$

(R is the sphere radius, k^{-1} the Debye length, ε the permittivity, and Z the particle charge)

Charge estimation: The ζ potential of charged spherical particle is expressed with Eq. 2:

The charge Z can be estimated from the pK of the analytes as a function of the pH with the Henderson–Hasselbalch equation. However for a series of analyzed components, the pK values found in literature databases are often not comparable or useable for the chosen experimental conditions (measured at different ionic strength, temperatures, or in different solvents). In this case, several simulation programs are available and can be used; some were tested within this study. Best results (relative values) are obtained when taking a homogeneous set of values (i.e., calculated with identical programs or from the same database).

Frictional coefficient (f) estimation: This parameter (f) corresponds to the drag (viscous) force the particle experiences when moving with a given velocity under an electrical field and its estimation is more ambiguous than for charge. An approach would be usable to derive it from the Nernst–Einstein equation:

$$D = \frac{kT}{f} \tag{3}$$

(D is the diffusion coefficient, k the Boltzmann constant, T the temperature)

$$\mu = \frac{qe}{kT} \times D \tag{4}$$

(k is the Boltzmann constant, T the temperature, z the charge, μ the mobility)

Because this relationship is rarely used, diffusion coefficients (D) can be determined [21] with Eq. 4 when the mobility and the charge are known:

$$f = 6\pi\eta R \tag{5}$$

(η is the viscosity, R the radius of the ion)

A first approximation of f can be used for spherical shaped and rigid ions through the Stokes Eq. 5:

$$\mu = \frac{qe}{6\pi\eta R} \tag{6}$$

This leads to mobility Eq. 6:

The resulting approximations, however, are very imprecise because R is often unknown and can only be determined on basis of diffusion, sedimentation, or electrophoretic mobility. Moreover,

the solvent/water and ions moving with the analyte are not taken into account. This effect can be estimated taking account of the Debye theory presented earlier and the nature of the solution contiguous to the ion (ionic strength, counterions). The ion cloud can influence the mobility and lead to *relaxation* effects. Cifuentes and Poppe (1997) combined the relaxation effects and electrophoretic retardation effects into a reducing effect on the mobility. They presented a model in which the effects of the deformation of the ion cloud around the moving ion was included and leads to formation of an electric force that counteracts the applied field [2]. In the case of large moving ions (compared to the buffer ions), the relation could be reduced to Eq. 7:

$$\mu = A \times \frac{qe}{6\pi\eta R^2} \tag{7}$$

(with A is a constant)

Theoretical approaches give much insight into the mobility of smaller ions, but fail for highly charged and larger ions. Following a more empirical approach is therefore often the best strategy [2].

3 Mobility Prediction from Structural Data

Many empirical models can be found in literatures that were developed that fit the experimental and predicted data for very specific compounds classes (mainly peptides). These mobility expressions usually include in the formula the charge (Z) of the analyte, its molecular mass (M), or the number of amino acids (n). These formulations include:

Grossman's Eq. (8) [4]:

$$\mu = A \times \frac{\log(Z+1)}{n^B} \tag{8}$$

(Z the charge, A and B are constants, n number of amino acids)

Offords approach (Eq. 9) [5, 19, 22]:

$$\mu = A \times \frac{Z}{M^{2/3}} \tag{9}$$

(Z the charge, A constants, M molecular mass)

$$\mu = A \times \frac{Z}{M^{\mathrm{m}}} \tag{10}$$

$$\mu = A \times \frac{Z}{BM^{1/3} + CM^{2/3}} \tag{11}$$

(Z the charge, A, B, C and m constants, M molecular mass)

Compton's Eqs. (10) and (11) [3, 20]:

Cifuentes and Poppe conducted this development further and came up with a relation giving the best mobility prediction for peptides (Eq. 12) with a combination of Eqs. 8 and 9 [1, 2, 23].

$$\mu = A \times \frac{\log(1 + BZ)}{M^{C}} \tag{12}$$

(Z is the charge, A and B are constants, M is the molecular weight)

An interesting approach is the one of Fu and Lucy [24] that integrated the effects of hydration using the McGovan hydration increments [25] to further improve the prediction. It is however limited to monoamines and the equations are far from being phenomenological.

4 Experimental Approach

4.1 A Semiempirical Model for Small Molecules

For the development of a general mobility model, we wanted to stay as close as possible to the phenomenological approach (Eq. 7). Any purely mathematical data linearization and curve fitting would improve the prediction but would limit the possibility of data interpretation with the particular samples used for the fitting (see equations earlier).

Originally we wanted to use the equation for anionic NOM (natural organic matter); we chose substances similar in structure and mobility, like phenolic, aliphatic, and sugar acids. The relation $\mu = f$(charge, size) had to be tested over different pH ranges to be able to interpret mobility changes versus pH as derived from charge and size effects.

The first problem was to find a homogeneous data set of pK values. The values found in literature often varied in the range of 50%, due to the use of different solvents and temperatures. We chose to simulate pK with three available pK-simulation software programs and to compare the obtained values within the phenomenological models. We estimated all pKs with the Pallas 3.1 [26], ACD-Labs pK calculator 3.5, and the SPARC chemical reactivity model (the latter was available thanks to Dr. S.W. Karickhoff, Dr. A.W. Garisson, and Dr. J.M. Long, USEPA Athens Georgia USA [27, 28]). For a given pH, different charged states are calculated in each of the three pK calculation possibilities; when calculating the hydration effect with the McGovan increment method this had to be taken in account.

The Stoke's radius can be obtained by treating the molecule as a sphere and using the van der Waals volumes calculated by molecular modeling (Alchemy III and ACD Sotware). From the volumes, the corresponding radii were calculated assuming spherical shapes. Since the size data obtained in this way is not always available, it was important to compare these models with systems using the molecular mass only.

The tested models are listed in Fig. 1. From all tested combinations (3 different p*K* sources, size modeled with *M*, *r*, *s*, *v* and the hydration effect H), we selected the one that gave the best regression coefficient. Hydration factors were calculated for each substance and added to the molecular weight (weight factor taken from the table in [25] as a function of the present structures (calculations needed to be done at each pH to take account of the partial ionization of the acidic groups) [24, 25]. These values are given in Table 1 for selected data combinations and include phenolic acids only. Other attempts to include additional molecular

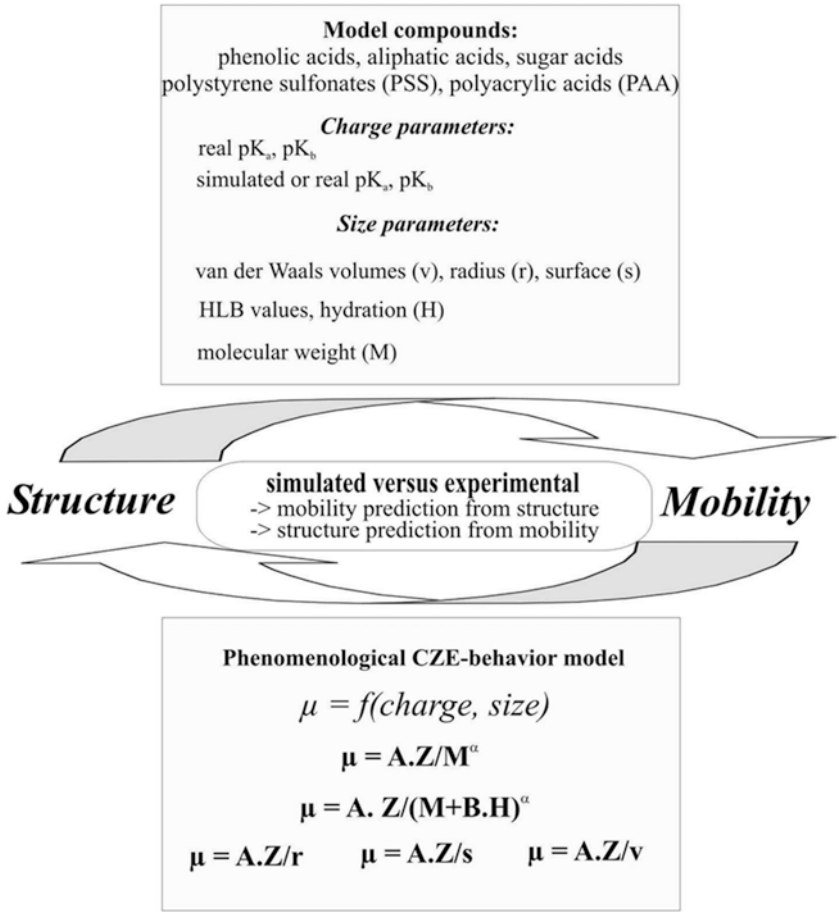

Fig. 1 The applied approach for the phenomenological model

Table 1

pK_a (calculated from the Pallas Software package) and molecular weight of selected aliphatic, phenolic, and sugar acids

Aliphatic acids	pK_a (Pallas)	Molecular weight	Phenolic acids	pK_a (Pallas)	Molecular weight
Formic acid	3.55	46.0	Phenol	9.92	94.1
Acetic acid	4.56	60.1	Catechol	9.53, 12.67	110.1
Oxalic acid	0.99, 6.68	74.0	Resorsinol	9.33, 11.27	110.1
Propionic acid	4.76	74.1	Benzoic acid	4.2	122.1
Glycolic acid	3.75	76.1	*o*-Hydroxybenzoic acid	4.07, 9.72	122.1
Butyric acid	4.63	88.1	Methylcatechol	9.96, 12.69	124.1
Pyruvic acid	2.26, 2.26	88.1	Transcinnamaldehyde	13.15	132.2
Glyoxylic acid	1.18	90.0	2,4-Hydroxybenzaldehyd	7.33, 9.3	138.1
Lactic acid	3.75	90.1	m-Hydroxybenzoic acid	2.66, 10.03	138.1
Valerianic acid	4.84	102.2	*p*-Hydroxybenzoic acid	4.58, 10.03	138.1
Malonic acid	2.77, 5.38	104.1	*p*-Hydroxyphenyl acetic acid	4.497.85	152.2
Glyceric acid	3.41	106.1	Protocatechoic acid	4.45, 9.94, 12.17	154.1
Fumaric acid	4.09, 4.69	116.1	alpha-Methylcinnamic acid	5.17	162.2
Levulinic acid	4.69	116.1	*m*-Coumaric acid	4.39, 9.59	164.2
Succinic acid	4, 5.24	118.1	*o*-Coumaric acid	4.63, 9.87	164.2
Erythronic acid-1,4-lacton	12.38	118.1	*p*-Coumaric acid	4.63, 9.58	164.2
Tartronic acid	2.31, 4.64	120.1	Phthalic acid	2.95, 5.41	166.1
Malic acid	3.16, 4.59	134.1	4-Tertiobuthylcatechol	10.03, 12.71	166.2
Threonic acid	3.86	136.1	Vanillic acid	4.47	168.2
Adipic acid	4.37, 5.06	146.2	Gallic acid	4.32, 8.86, 10.68	170.1
Tartaric acid	2.7, 3.99	150.1	Ascorbic acid	3.94, 12.78	176.1
Galactonic acid-1,4-lacton	12.13	178.2	*t*-3,4,-Dimethoxycinamic acid	4.54	176.2

(continued)

Table 1
(continued)

Aliphatic acids	pK_a (Pallas)	Molecular weight	Phenolic acids	pK_a (Pallas)	Molecular weight
Isosacharin	3.19	180.2	4-Hydroxy, 3-methoxycinamaldehyde	9.63, 13.31	178.2
Citric acid	2.39, 4.01, 4.9	192.1	Coffeic acid	4.57, 9.5, 12.04	180.2
Mannonic acid-1,4-lactone	3.16, 12.73	192.1	Coniferyl alcohol	10.09	180.2
2-Keto-gluconic acid	3.08	194.1	Homovanillic acid	4.43, 7.85	182.2
5-Keto-gluconic acid	3.26	194.1	Ferulic acid	4.58, 9.58	194.2
Gluconic acid	3.27	196.2	Syringic acid	4.36, 10.03	198.2
Galactaric acid	2.92, 3.63	210.2	Trimellitic acid	2.81, 4.16, 4.76	210.1
Glucaric acid	2.92, 3.64	210.2	2,6-Naphthalene dicarboxylic acid	3.67, 4.51	216.2
			Sinapic acid	4.53, 9.58	224.2
			Pyromellitic acid	1.86, 3.03, 4.5, 5.67	254.2
			Quercetin	8.9, 9.95, 11.23, 12.83	302.2
			Conidendrin	9.8, 10.36	356.4
			Matairesinol	9.98, 10.06	358.4
			Pinoresinol	9.92, 10.53	358.4
			Hydroxymatairesinol	9.95, 10.05	374.4
			Rutin	8.92, 10.1, 11.38, 12.63	610.5

characteristics such as the hydrophobicity (Log*P*) or the ovality of the molecules were not successful.

The requirement to the separation buffer was to be noncomplexing toward the analytes so that the measured mobility could be attributed to structural effects only. Borate is, for example, a buffer that interacts with diol groups and therefore induces some mobility shifts as a function of the binding strength. For all the tested combinations, we compared the experimental data (all data sets were

Table 2

Selected best R^2 results from the data linearization using different models for charge (pK_a from ACD, Pallas, SPARCS) and size (molecular weight Mw, van der Walls radius r^2, hydration factor H corrected van der Waals radius R^2)

					H from ACD		H from SPARC		H from PALLAS	
pK_a\Size	$Mw^{2/3}$	$Mw^{2/3}$ hydr. Corrected	r^2 Alchemy	r^2 ACD	hydr. R^2 Alchemy	hydr. R^2 ACD	hydr. R^2 Alchemy	hydr. R^2 ACD	hydr. R^2 Alchemy	hydr. R^2 ACD
ACD	0.9151	0.8689	0.9146	0.8847	0.8776	0.8747	0.8587	0.853	0.8581	0.8522
SPARC	0.94	0.8786	0.9395	0.9163	0.8754	0.8761	0.8866	0.8877	0.861	0.8599
PALLAS	0.9384	0.9134	0.9355	0.9097	0.9191	0.9187	0.9086	0.907	0.9213	0.9208

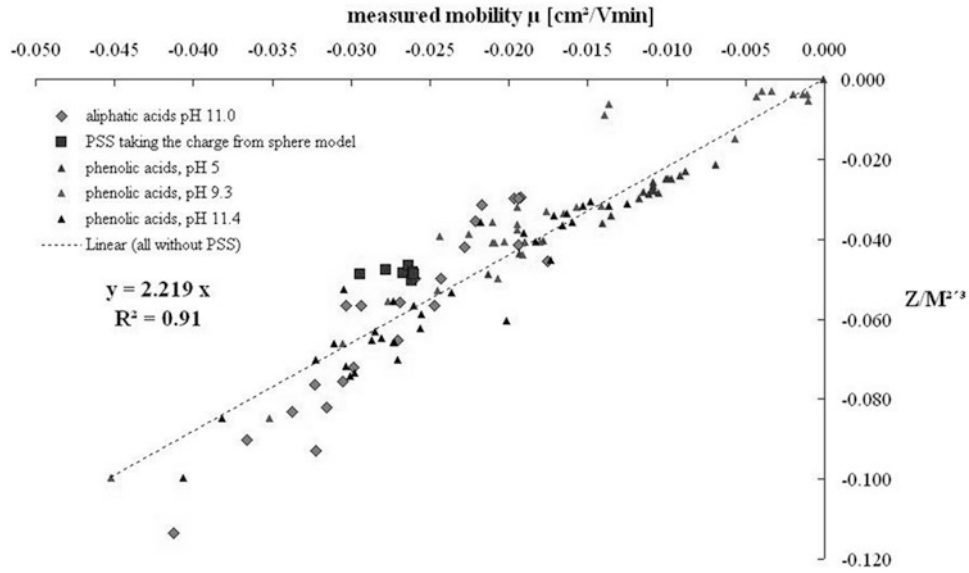

Fig. 2 All experimental data sets involving phenolic acids at three different pH and aliphatic acids at pH 11

calculated with the phenolic compounds at three pHs) with simulated mobility values involving the van der Waals volumes/surface/radius and additional hydration volumes. The simplest model (already proposed by Offord in 1966) was found to be the best with a linearity of $R^2 = 0.9384$ (*see* Table 2).

Including the experimental data of the aliphatic acids into the Offord model, the data also fit into the linearity (Fig. 2). Aliphatic acids were measured at pH 11.0 using CTAB to invert the EOF and 2,6-naphthalenedicarboxylic acid as a UV absorbing background electrolyte [29]. Acetic acid was used as an internal standard for mobility correction.

The shape and the size of the molecules are thus directly responsible for their mobility. Assuming a homogeneous density of the molecules and a spherical shape, the radius is proportional to the power of 1/3. This hypothesis was verified for all the model phenolic acids studied earlier and found the relation ($r = 0.59385.\ M^{1/.3}$ with $R^2 = 0.901$), where r was obtained from the calculated volumes of the phenolic acids with Alchemy 2000 software.

When substituting this relation in the Stoke's Eq. 6, the proportionality of the mobility to $M^{-2/3}$ is verified. It was also found previously by many authors that Offord's model is verified for peptides [2, 5, 22].

This result signifies that surface charge density governs the mobility of these analytes. However, a universal model could never been verified between all available data sets because the dependency on $M^{-\alpha}$ (α between 1/3 and 2/3) was a function of the used amino acid residues and the composition of the separation buffer (complexing or noncomplexing, ionic strength effects on the Debye length). In the studies presented here, we systematically used noncomplexing (acetate and carbonate buffers) at the same ionic strength (25 mM) and in all calculations structural data was used from the same source (identically simulated).

This best empiric relation for mobility found with all tested combinations, which can systematically be used in CZE method developments is:

$$\mu = A \times \frac{Z}{M^{2/3}} \tag{13}$$

with $A = 2.219$ in our experimental conditions for these analytes.

More information on mobility variation with pH is gained with this approach than using the simple relation between the mobility and the pK of the substances, which can only be taken as a preliminary assessment of separation [30]. The Offord model can be used in a general manner to simulate systematically the electrophoretic mobility of the components of interest over the pH range. An example of theoretical evolution of the mobilities by pH is illustrated for aliphatic and phenolic acids in Fig. 3. Different pH zones can be differentiated (arrows) in which the mobilities of the components are governed alone by COOH groups (carboxylic acidity, pH 5) or OH and COOH group (total acidity, pH 11.4). At a pH around 9, the phenols (low mobility) can be additionally distinguished from the phenolic acids (high mobility).

4.2 Simulation and Separation of Hydroxy-s-Triazines as Cations and Anions in CZE

An example of the application of this approach is given for the optimization of the separation of 12 hydroxy-s-triazines, all hydroxylated metabolites of s-triazine pesticides presenting different side chain substituents (Table 3). Based on Eq. 13, the pK_a and the molecular mass values in Table 3, an evolution of the

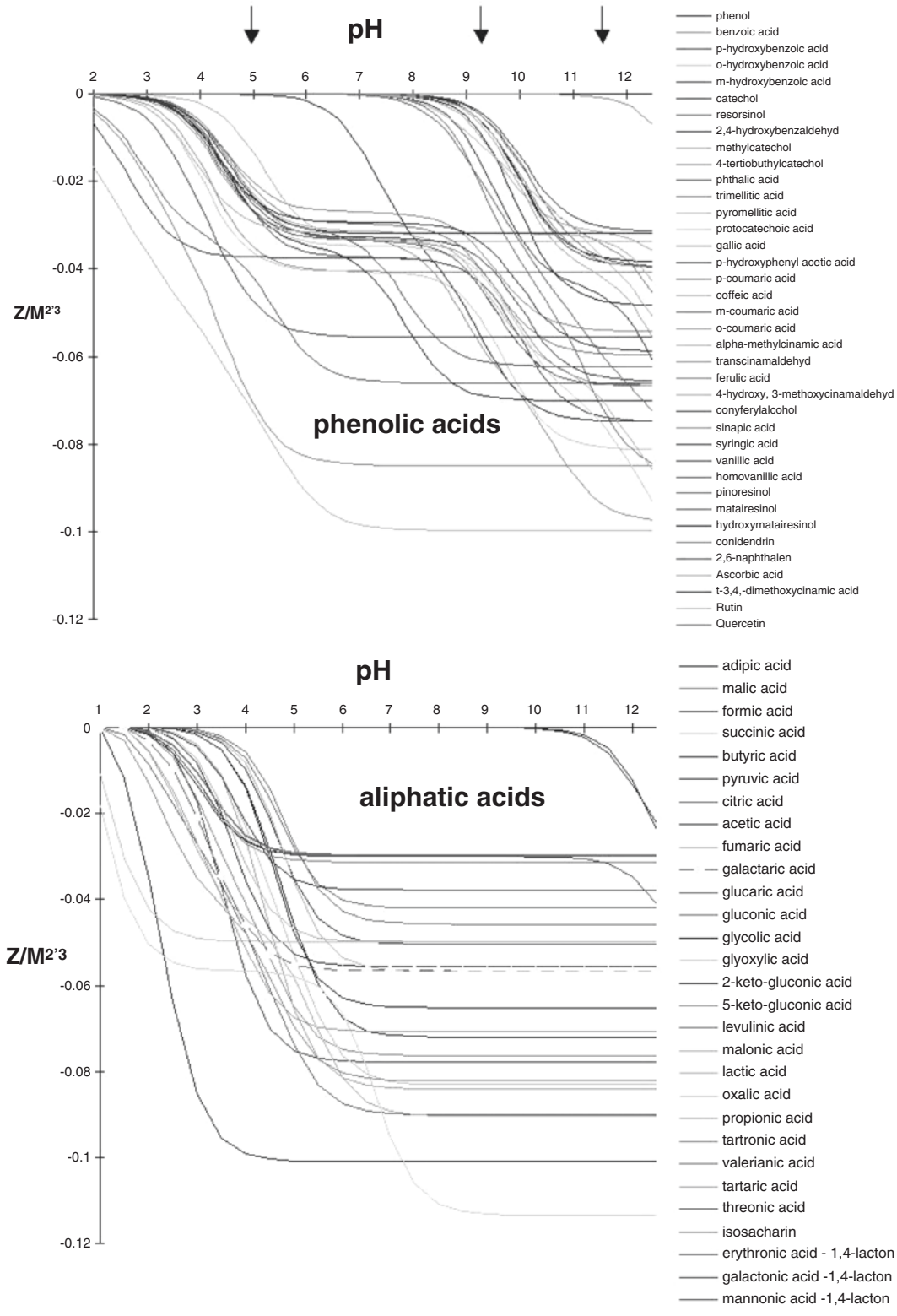

Fig. 3 Theoretical mobility evolution by pH using the Offord model for phenolic and aliphatic acids. Important in this figure is not to recognize the different traces but actually to see the potential of the simulation in rapidly recognizing the best pH for the optimal separation of components in mixtures

Table 3

Substituted hydroxy-s-triazines (1-12 in Fig. 4), their mass *M* and acidic pK_a and basic pK_b

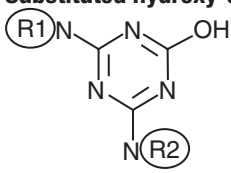

R1, R2		M	pK_a	pK_b
H, H	1	127	4.44	9.54
H, Et	2	155	4.64	9.93
H, iPr	3	169	4.71	9.96
H, tBu	4	183	4.91	10.34
Et, Et	5	183	4.94	10.31
H, mAr	6	233	3.96	9.48
Et, iPr	7	197	4.95	10.39
Et, tBut	8	211	5.2	10.88
iPr, iPr	9	211	5.01	10.88
iPr, Ar	10	245	4.24	9.78
H, Ar	11	203	4.02	9.49
iPr, mAr	12	275	4.29	9.73

theoretical mobility can be calculated as a function of pH. The resulting curves are shown in Fig. 4.

From Fig. 4 it can easily been seen that the optimum separation pH is at low or high pH values; at neutral pH the mobility of the analytes is zero (all analytes migrate with the EOF) due to the zwitterionic character of the substances. Indeed the electropherograms shown in Fig. 4 verify nicely this separation selectivity.

Actually the knowledge of the variations in electrophoretic mobility by pH can be used to determine precisely pK_a values as illustrated with the same analytes in ref. [14] and in the review chapter on pharmaceuticals of Marsh et al.

4.3 Confirmation of Aminoalcohol in the CZE-Indirect Detection of Formaldehyde Releasers

Unsaturated triazines and oxasolidines used as biocides in metalworking fluid were separated at neutral pH condition since they are not stable under acidic medium; they hydrolyze releasing formaldehyde and different derivatives of corresponding aminoalcohols. According to Offord's model, the $Z/M^{2/3}$ values of the analytes calculated at pH 7 are differed from each other, meaning that they can be separated with capillary electrophoresis. However after separation with a noncomplexing buffer, the measured mobilities did

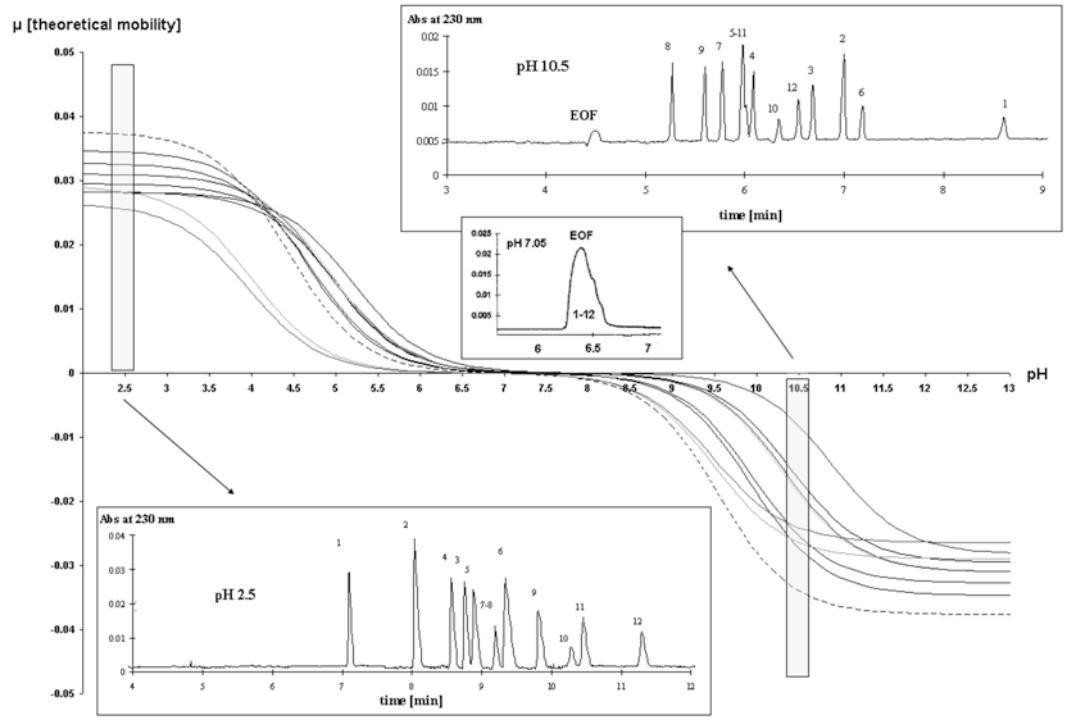

Fig. 4 Theoretical evolution of the mobility by pH for the substituted hydroxy-s-triazines in Table 3

not check up with the corresponding $Z/M^{2/3}$ values (all measured mobilities were much lower than the estimated ones). Moreover, two substances migrated together in spite the fact that their calculated $Z/M^{2/3}$ was totally different (linear correlation between the theoretical and measured values was as low as $r^2 = 0.320$). Since the hydrolysis products of these two analytes are identical we calculated the $Z/M^{2/3}$ of all possible aminoalcohols and compared them to their measured mobility. Strong linear correlation ($r^2 = 0.995$) was found between the calculated and measured mobility of the aminoalcohols as shown in Fig. 5.

Thus, applying this semiempirical approach it was possible to verify that the selected hexahydro-triazines and oxasolidines were rapidly hydrolyzed under the separation condition and thus the hydrolysis products were detected. This hypothesis was verified with CE/MS and NMR studies not shown here. Consequently, these biocides can be indirectly identified with capillary electrophoresis if the sample does not contain the hydrolysis product (derivatives of aminoalcohols).

5 Conclusion

The Offord model (effective mobility linearly correlated to $Z/M^{2/3}$) was verified as the simplest and most accurate approach to rapidly simulate the relative mobility of ions in free zone electrophoresis

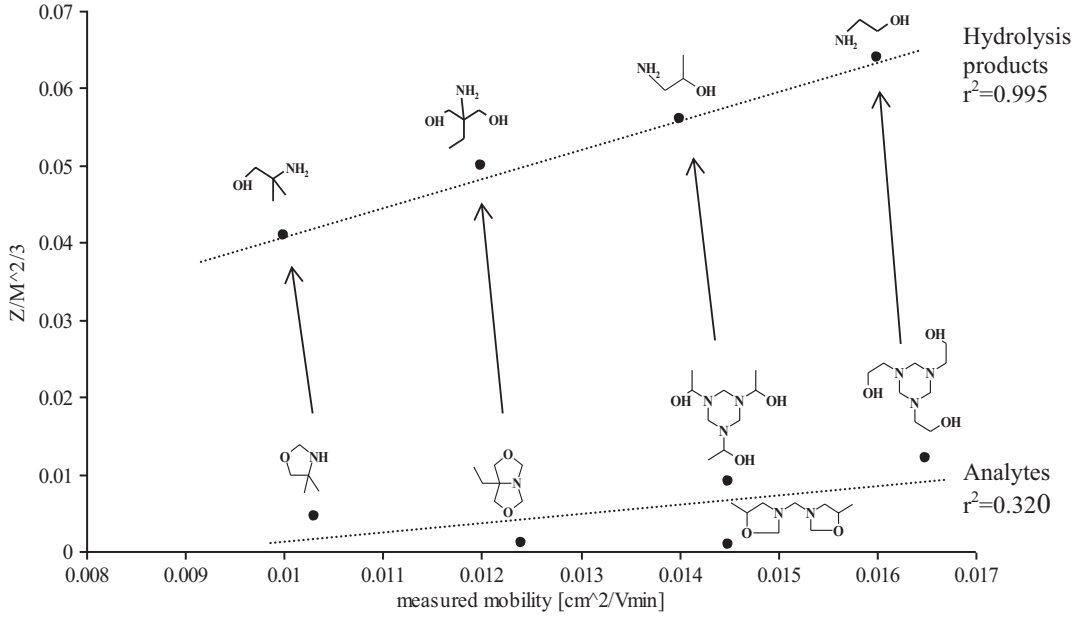

Fig. 5 Comparison of the measured mobility and Offord model ($Z/M^{2/3}$) of the selected unsaturated triazines and oxasolidines and their hydrolysis products

based on their chemical structure. The charge can easily be calculated from the p*K* values (as from the literature, databases, or calculated by simulation programs) and the mass can be used to evaluate the frictional force. The accuracy of the model is robust enough to give at least a good estimation of a starting pH when developing methods to separate known substances in mixtures or to confirm charge-to-mass ratios of known/unknown structures in method development.

Acknowledgement

H. Neumeir and B. Look are thanked for their technical assistance and their kind support during the past years.

References

1. Cifuentes A, Poppe H (1995) Effect of ph and ionic strength of running buffer on peptide behavior in capillary electrophoresis: theoretical calculation and experimental evaluation. Electrophoresis 16:516–524
2. Cifuentes A, Poppe H (1997) Behavior of peptides in capillary electrophoresis: effect of peptide charge, mass and structure. Electrophoresis 18:2362–2376
3. Chen N, Wang L, Zhang YK (1993) Correlation free-solution capillary electrophoresis migration times of small peptides with physicochemical properties. Chromatographia 37:429–432
4. Grossman PD, Colburn JC, Lauer HH (1989) A semiempirical model for the electrophoretic mobilities of peptides in free-solution capillary electrophoresis. Anal Biochem 179:28–33

5. Rickard EC, Strohl MM, Nielsen RG (1991) Correlation of electrophoretic mobilities from capillary electrophoresis with physicochemical properties of proteins and peptides. Anal Biochem 197:197–207
6. Havel J, Janos P (1997) Evaluation of capillary zone electrophoresis equilibrium data using the CELET program. J Chromatogr A 786:321–331
7. Britz-McKibin P, Chen DDY (1997) Prediction of the migration behavior of analytes in capillary electrophoresis based on three fundamental parameters. J Chromatogr A 781:23–34
8. Sahota RS, Khaledl MG (1994) Target factor modeling of migration behavior in capillary electrophoresis. Anal Chem 66:2374–2381
9. Ermakov SV, Bello MS, Righetti PG (1994) Numerical algorithms for capillary electrophoresis. J Chromatogr A 661:265–278
10. Gas B, Vacik J, Zelensky I (1991) Computer-aided simulation of electromigration. J Chromatogr 545:225–237
11. Kohlrausch F (1897) Ueber Concentrations-Verschiebungen durch Electrolyse im Inneren von Lösungen und Lösungsgemischen. Annalen der Physik und Chemie B 62:210–239
12. Ermakov SV, Mazhorova OS, Zhukov MY (1992) Computer simulation of transient states in capillary zone electrophoresis and isotachophoresis. Electrophoresis 13:838–848
13. Gluck SJ, Steele KP, Benkö MH (1996) Determination of acidity constants of monoprotic and diprotic acids by capillary electrophoresis. J Chromatogr A 745:117–125
14. Schmitt P, Poiger T, Simon R, Garrison AW, Freitag D, Kettrup A (1997) Simultaneous ionization constants and isoelectric points determination of 12 hydroxy-s-triazines by capillary zone electrophoresis (CZE) and capillary electrophoresis isoelectric focusing (CIEF). Anal Chem 69:2559–2566
15. Freitag D, Schmitt-Kopplin P, Simon R, Kaune A, Kettrup A (1999) Interactions of hydroxy-s-triazines with SDS-micelles by micellar electrokinetic capillary chromatography (MEKC). Electrophoresis 20:1568–1577
16. Gao J, Gomez FA, Härter R, Whitesides GM (1994) Determination of the effective charge of a protein in solution by capillary electrophoresis. Proc Natl Acad Sci 91:12027–12030
17. Menon MK, Zydney AL (1998) Measurement of protein charge and ion binding using capillary electrophoresis. Anal Chem 70:1581–1584
18. Schmitt P, Trapp I, Garrison AW, Freitag D, Kettrup A (1997) Binding of s-triazines to dissolved humic substances: electrophoretic approaches using affinity capillary electrophoresis (ACE) and micellar electrokinetic chromatography (MEKC). Chemosphere 35:55–75
19. Offord RE (1966) Electrophoretic mobilities of peptides on paper and their use in the determination of amide groups. Nature 211:591
20. Compton BJ (1991) Electrophoretic modeling of proteins in free solution zone capillary electrophoresis and its application to monoclonal antibody microheterogeneity analysis. J Chromatogr 559:357
21. Nikodo AE, Garnier JM, Tinland B, Ren H, Desruisseaux C, McCormick LC, Drouin G, Slater GW (2001) Diffusion coefficient of DNA molecules during free solution electrophoresis. Electrophoresis 22:2424–2432
22. Cross RF, Cao J (1997) Salt effects in capillary zone electrophoresis 1. Dependence of electrophoretic mobilities upon the hydrodynamic radius. J Chromatogr A 786:171–180
23. Cifuentes A, Poppe H (1994) Simulation and optimization of peptide separation by capillary electrophoresis. J Chromatogr A 680:321–340
24. Fu S, Lucy CA (1998) Prediction of electrophoretic mobilities. 1. Monoamines. Anal Chem 70:173–181
25. McGowan JC (1990) A new approach for the calculation of HLB values of surfactants. Analyse 27:229–230
26. Fekete J, Morovjan G, Csizmadia F, Darvas F (1994) Method development by an expert system: advantages and limitations. J Chromatogr A 660:33–46
27. Hilal SH, Karickhoff SW (1995) A rigorous test for SPARC's chemical reactivity models: estimation of more than 4300 ionization pk_as. Quant Struct Act Relat 14:348–355
28. Karickhoff SW, McDaniel VK, Melton C, Vellino AN, Nute DE, Carreira LA (1991) Predicting chemical reactivity by computer. Environ Toxicol Chem 10:1405–1416
29. Dabek-Zlotorzynska E, Dlouhy JF (1994) Capillary zone electrophoresis with indirect UV detection of organic ions using 2,6-naphthalenedicarboxylic acid. J Chromatogr A 685:145–153
30. Souza SR, Tavares MFM, de Carvalho LRF (1998) Systematic approach to the separation of mono- and hydroxycarboxylic acids in environmental samples by ion chromatography and capillary electrophoresis. J Chromatogr A 796:335–346

http://www.springer.com/978-1-4939-6401-7

Capillary Electrophoresis
Methods and Protocols
Schmitt-Kopplin, P. (Ed.)
2016, XI, 527 p. 156 illus., 28 illus. in color., Hardcover
ISBN: 978-1-4939-6401-7
A product of Humana Press